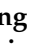*Article*

The Variation in Boulder Bars Triggered by the 2018 Sedongpu Natural Dam Failure in the Yarlung Tsangpo River

Xiangang Jiang [1,2,3,*], Xinlin Xie [1], Zhehao Guo [1], Anders Wörman [4], Xingrong Liu [5], Weiming Liu [2] and Yiqin Xie [6]

1   College of Civil Engineering, Sichuan Agricultural University, Chengdu 611830, China; 2022326035@stu.sicau.edu.cn (X.X.); guozhehao@stu.sicau.edu.cn (Z.G.)
2   CAS Key Laboratory of Mountain Hazards and Surface Process, Institute of Mountain Hazards and Environment, Chinese Academy of Sciences (CAS), Chengdu 610041, China; liuwm@imde.ac.cn
3   PowerChina Kunming Engineering Co., Ltd., Kunming 650233, China
4   Division of River Engineering, Royal Institute of Technology, 100 44 Stockholm, Sweden; worman@kth.se
5   Geological Hazards Prevention Institute, Gansu Academy of Sciences, Lanzhou 730000, China; liuxr_2024@163.com
6   Key Laboratory of Sediment Science and Northern River Training, The Ministry of Water Resources, China Institute of Water Resources and Hydropower Research, Beijing 100080, China; xieyq@iwhr.com
*   Correspondence: jxgjim@163.com

Abstract: Natural dams are formed most often in narrow, steep valleys in high mountains. The outburst floods triggered by natural dam failures result in the topography and landforms successively being altered. Boulder bars are common natural structures that are selected here to quantitatively evaluate the impact of outburst floods on the topographical and landform variations in downstream channels. In this study, we selected the Sedongpu natural dam on the Yarlung Tsangpo River formed as a result of a landslide in 2018 as an example, and studied the geomorphological changes in a river reach located 173 km downstream of the Sedongpu natural dam. The sizes and shapes of the boulder bars in this area were statistically analyzed. The results show that there are three shape types of boulder bars in this area, i.e., sickle, bamboo leaf and oval. Furthermore, it found that the relationship between the lengths and widths of boulder bars is similar before and after outburst floods, as is the relationship between perimeters and lengths of boulder bars, which means these relationships are not affected by outburst floods. And the perimeters of boulder bars are almost twice their lengths. In addition, the relationship between the areas and lengths of boulder bars follows a power function. The most important finding is that the riverine morphological features conserved self-similarity due the influence of the outburst flood erosion triggered by a natural dam failure. This finding adds to the previous observations since dam failures introduce sudden and dominating impacts on river systems.

Keywords: natural dam; boulder bar; evolution mode; outburst flood

1. Introduction

Occasionally, the water stored in a dam reservoir can be released suddenly due to a dam burst, creating a large-scale burst flood [1–5]. These large-scale outburst floods have significant entrainment effects on riverbeds [6]. For example, they can erode and scour both bedrock and soils and lead to alterations in the topography of the original river course. These effects can even cause the disappearance of certain landforms present in the original river channel. In addition, these outburst floods can transport sediments from upstream, which are mainly bed loads, which, once they reach the terraces of riverbanks, will accumulate and change the topography and landforms of the riverbanks [7–9].

A boulder bar is an accumulated river landform that appears in the river channel and along the riverbanks. The sizes or shapes of boulder bars can be changed by erosion or deposition around them due to outburst floods [10]. Therefore, a boulder bar is a reference

that reflects the impact of outburst floods on the topography and geomorphology of river courses. The sizes of boulder bars are directly affected by the velocities and water levels of floods; that is, boulder bars can be altered slightly by outburst floods with low velocities and low water levels. Meanwhile, under conditions of rapid currents and high-water levels, boulder bars will be strongly eroded and even destroyed due to the action of bursting floods. Furthermore, new boulder bars may be formed downstream due to the same action [11]. In addition, the sizes of the sediment particles that are carried by burst floods also affect the sizes of boulder bars. In general, the transported sediments with coarser particles have a dominant effect on the shapes and sizes of boulder bars, while smaller particles are more likely to settle and accumulate around the boulder bars, increasing their sizes [12–14].

Floods that are caused by natural dam failures are a common type of flooding in river basins. Many cases have shown that outburst floods triggered by natural dam bursts can change the sizes and shapes of boulder bars downstream [10,11]. For example, Wu et al. [11] selected a research area located 17 km downstream of Yigong Barrier Lake and found that outburst floods were responsible for a reduction in the area of boulder bars in the study area. However, these studies analyzed only the areas, lengths and widths of boulder bars, and the quantitative relationships among these different parameters were not examined. In particular, there is a lack of comparative analyses of the sizes of boulder bars before and after natural dam failures. In addition, the variation modes of boulder bars after a natural failure are also an interesting topic, but they have not been reported in the literature.

The topography of fluvial erosion has often been cited as an example of self-similarity in nature [15,16]. This indicates that riverine geometric structures conserve self-similar shapes for long-term fluviation. Transient river dynamics, such as a sudden and dominant impact of outburst floods on river systems, followed by an accumulation of sediments or adjustment of bed topography, typically exhibit both translation and dispersion [17]. Whether self-similarity still exists in the stream bed topography after this transient process is still unclear. Hence, the objectives of our research are to show how a natural dam failure influences downstream riverine morphological features and whether the bedform features take self-similar shapes, as found in previous research. For this, a 173 km section of the downstream river channel of the Sedongpu natural dam was taken as the research area.

The Sedongpu natural dam occurred in the Sedongpu Basin, with a landslide volume of 3000×10^4 m^3, on the 29 October 2018. The fundamental cause of this event was the collapse of a glacier. The collapse occurred approximately 6 km upstream in the Sedongpu Basin at an elevation of 4070 m [18]. During the collapse process, part of the glacier detached and carried rocks and debris from the sides of the valley and the base of the glacier. Carrying ice and debris from the glacier, the mixture rushed down the valley. The snow and debris moved rapidly towards the bottom of the valley, traveling a long distance before entering the Yarlung Tsangpo River and colliding with the right bank, ultimately blocking the Yarlung Tsangpo River and forming a dam. The dam was approximately 2.5 km long, with a width ranging from 415 to 620 m and an area of approximately 1.29 km^2, with a volume ranging from 33 to 45×10^6 m^3 [18]. The Shedongpu natural dam was mainly composed of gravel and fine soil, with a small amount of snow, and a few boulders. The backwater in the upper reaches of the dam seriously threatened the road water conservancy facilities, electric power communication facilities and cultivated land in Gara Village, Blunt Village and Chibai Village in Tibet. The ratio of soil to rock was approximately 8:2 [19]. The natural dam breached in approximately 2 days [18]. The dam failure seriously damaged downstream Medog County and the Medog Yarang Hydropower Station. And 16,600 people were affected, 0.34 km^2 of arable land was affected, 7 km of road was damaged, and the preliminary estimate of economic loss was more than CNY 3×10^8.

In this study, the sizes of boulder bars, such as their lengths, widths, areas and perimeters, were compared before and after the failure of the Sedongpu natural dam combined with remote sensing images of the study area. And the number variation of

boulder bars after the dam failure was studied. In addition, the evolutionary pattern of boulder bars in the study area was investigated and summarized. Furthermore, the most important finding is self-similarity of riverine morphological features before and after the natural dam failure. This finding supplement previous observations, as the dam failure had a sudden and significant impact on the river system.

2. Materials and Methods

2.1. Study Area and Data

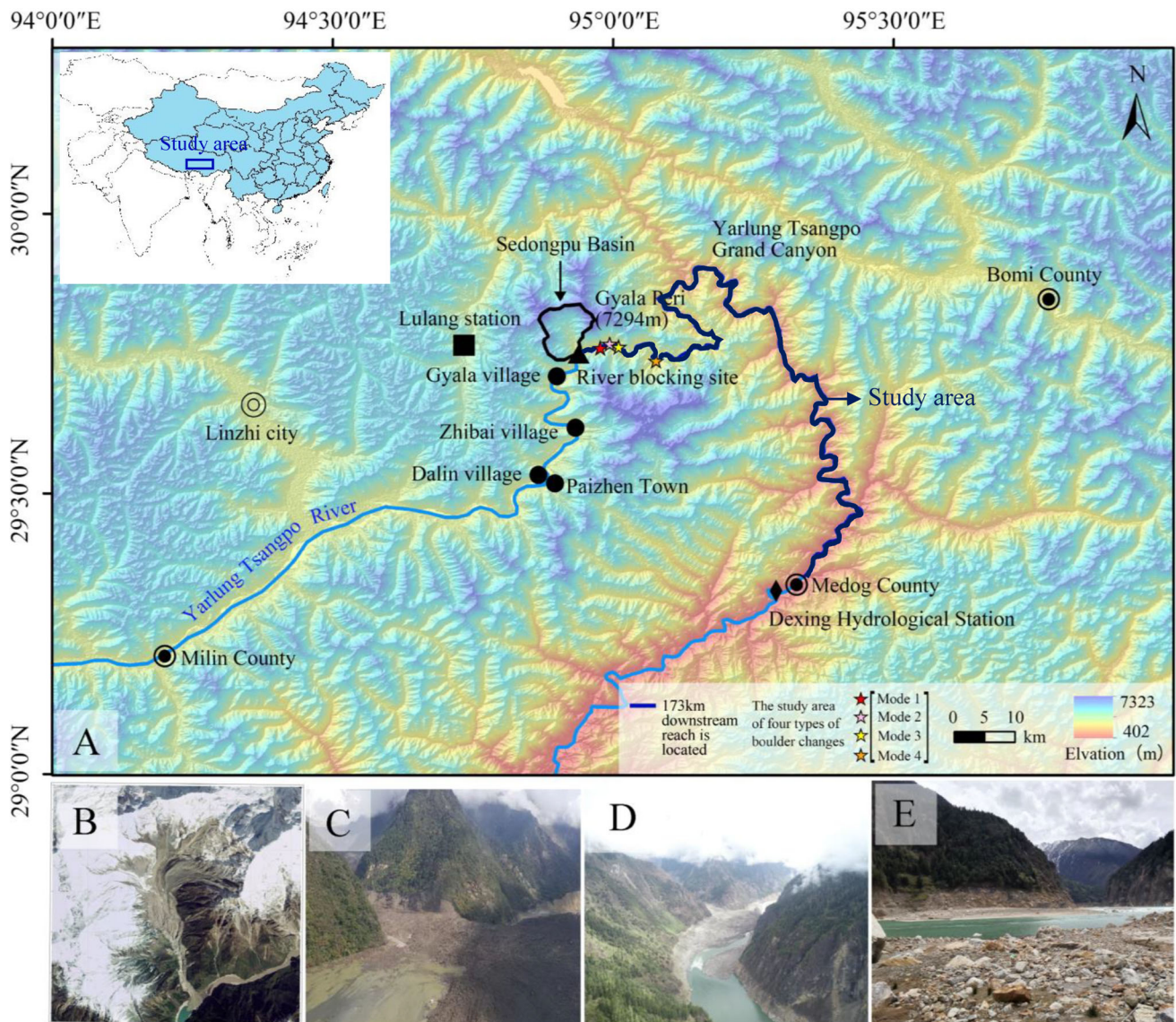The location of the Sedongpu natural dam and the general situation before and after dam failure are shown in Figure 1.

Figure 1. Study area and the Sedongpu natural dam. (**A**) The study area. The river portion located 173 km downstream from the Sedongpu natural dam was the study range. (**B**) An image of Sedongpu Basin and a map showing river blockages (created with the 0.8 m data of Beijing No. 2 on 31 October 2018). (**C**) The Sedongpu natural dam before failure (taken on 17 October 2018). (**D**) The Sedongpu natural dam after failure. (**E**) The boulder bars near the natural dam.

For this study, the topographical data of the 173 km long (L_T) river channel (study area) located downstream of the Sedongpu natural dam before (October 2018) and after (October 2020) the dam failure were obtained from Landsat 8 remote sensing images. The river

valley in the research area is narrow, with a width of 150–300 m and a "V" shape. There are 1–2 levels of terraces, with a height difference of around 1–3 m between terraces. The elevation of the terraces is 2710–2750 m. The lithology is mainly schist, gneiss, granulite, mixed rock, etc., which are often interbedded and prone to collapse and sliding. They are easily broken by glacier erosion and freeze–thaw weathering. The research area is a strong crustal activity zone characterized by compression, rotational strike slip and uplift, and is also prone to geological disasters such as landslides, mudslides and ice-rock collapses. In the 173 km river course, there were 104 boulder bars before the dam burst and 67 boulder bars after the dam burst. Furthermore, the lengths, widths, perimeters and areas of the boulder bars were measured. By comparing the shapes of the boulder bars before and after the failure of the Sedongpu dammed lake, the evolution modes of the boulder bars that were triggered by outburst floods could be summarized.

2.2. Method

Geometric Parameters Used for Boulder Bar Analysis

To determine the relationship between the boulder bar sizes, some dimensionless numbers are defined.

The first dimensionless number is Equation (1):

$$\lambda = \frac{L}{W} \tag{1}$$

where L and W are the length and width of the boulder bar, respectively.

To investigate the relationship between the perimeter (P), area (A) and L of the boulder bars, we define another two dimensionless numbers as Equation (2):

$$\alpha = \frac{P}{W} \tag{2}$$

and Equation (3):

$$\beta = \frac{A^{\frac{1}{2}}}{W} \tag{3}$$

The correlation coefficient is used here to investigate the relevance of two boulder bar parameters, as shown in Equation (4):

$$P_{XY} = \frac{Cov(X, Y)}{\sqrt{D(X)}\sqrt{D(Y)}} \tag{4}$$

where P_{XY} is the correlation coefficient; $Cov(X, Y)$ is the covariance; $D(X)$, $D(Y)$ are the variance of two groups of data, and X and Y are the evaluation data.

The standardized residual SR is used here to investigate the degree of dispersion of the geometric parameters of the distributed boulder bars. In general, the SR values form a normal distribution, and approximately 68% and 95% of the SR values are in [−1, 1] and [−2, 2]. The SRs follow Equation (5):

$$SR = \frac{y - \hat{y}}{S_{y-\hat{y}}} \tag{5}$$

where y is the measured value, $\hat{y}$ is the predicated value, and $S_{y-\hat{y}}$ is the standard deviation of residuals.

3. Results

3.1. Morphological Characteristics of Boulder Bars

Before the dam failure, the lengths of the boulder bars ranged from 62.7 m to 2195 m, the widths of the boulder bars ranged from 15.69 m to 238 m, the perimeters of the boulder bars ranged from 163 m to 4450 m, the areas of the boulder bars ranged from 1211 m^2 to

228,447 m^2, and the flatness of the boulder bars ranged from 3.5% to 97.7%. After the dam failure, the lengths of the boulder bars ranged from 77.23 m to 2357 m, the widths of the boulder bars ranged from 24.5 m to 203 m, the perimeters of the boulder bars ranged from 183.88 m to 4904 m, the areas of the boulder bars ranged from 1994.2 m^2 to 335,213 m^2, and the flatness of the boulder bars ranged from 36.6% to 95.8%.

The shapes of the boulder bars in the study area can be divided into three types: (1) The sickle type: the boulder bar bodies bend towards the convex bank of the river, the boulder bar heads (upstream of the boulder bar) are slightly blunt, and the boulder bar tails (downstream of the boulder bar) are sharpened like a sickle. (2) The bamboo leaf type: the edges of the boulder bar are smooth, and the boulder bar heads are blunt, short and thick, while the boulder bar tails are sharp and elongated, similar to bamboo leaves. (3) The oval type: the boulder bars have smooth borders that are wide in the middle and narrow at both ends, similar to an ellipse (Figure 2).
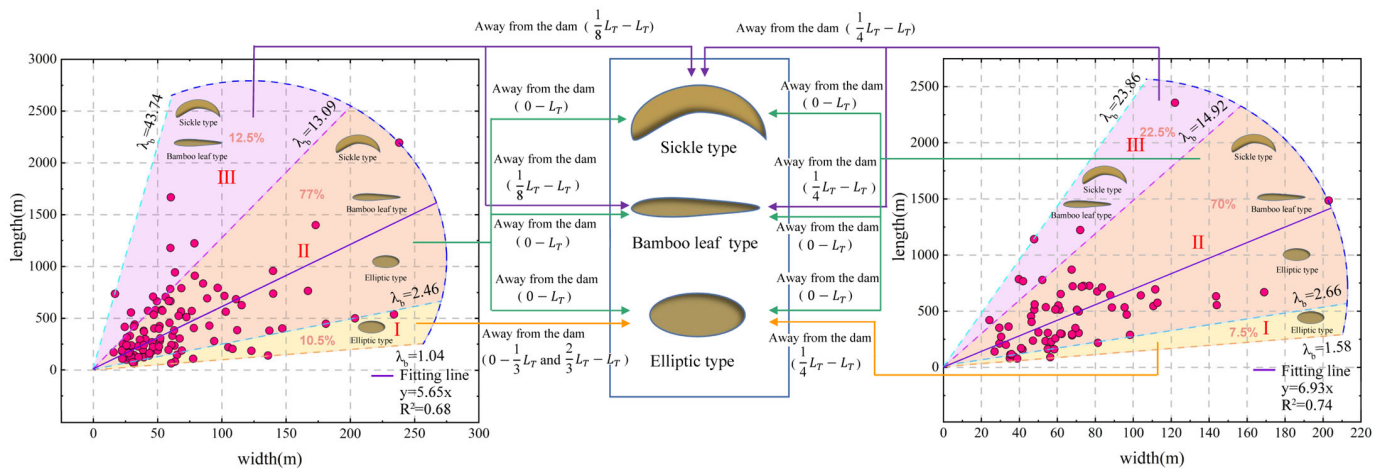

Figure 2. The relationships between the boulder bar lengths and widths (**left** figure: before the natural dam failure. **Middle** figure: the boulder bar shapes. **Right** figure: after the natural dam failure). L_T is the distance from the natural dam. λ_b is the aspect ratio of the boulder bar.

The remote sensing images indicate that the sickle-shaped boulder bars are mostly located in the curved parts of the river courses. The bamboo-leaf boulder bars are relatively large in length and width. These are a stable type of boulder bar. They are mostly located on the edges of the river. Elliptical boulder bars generally have small areas and are mostly located near dams and in the middle of river channels. They can be considered as the early form of boulder bars.

3.2. The Relationship between the Lengths and Widths of Boulder Bars

Figure 2 shows that before the failure of the Sedongpu natural dam, the boulder bars in the study area were within an interval of $\lambda \in [1.04, 43.74]$. Moreover, 95% of the boulder bars were less than 1000 m in length and less than 100 m in width. From a data distribution perspective, the lengths and widths of the boulder bars are linearly positively correlated.

Three *SR* intervals, namely ($SR < -1$), ($-1 \leq SR \leq 1$) and ($1 < SR$), were used to discriminate the dispersion degree of the data from the fitting curve in Figure 2. The λ values at the boundaries (λ_b) of the three internals were 2.46 and 13.09. The boulder bars with a small $\lambda \in [1.04, 2.46]$, falling in interval I, accounted for 10.5%, some of which were located within 1/3 L_T from the Sedongpu natural dam, and some within 2/3 L_T–L_T. The boulder bars at $\lambda \in [2.46, 13.09]$ falling in interval II, which accounted for 77%, were distributed throughout the entire study area. Boulder bars with $\lambda(\lambda \in [13.09, 43.74])$, accounting for 12.5% and falling in interval III, were mainly distributed within 1/8 L_T–L_T downstream of the Sedongpu natural dam, and most of them were present in the curved parts of river channels.

After the Sedongpu natural dam failure, the λ values were found to be in the range of [1.58, 23.86], and 94% of the boulder bars were less than 1000 m in length and less than 100 m in width. Similar to those before the failure of the Sedongpu natural dam, the lengths and widths of boulder bars have a linear positive correlation. As noted above, the boulder bars with small λ values ([1.58, 2.66]), falling in interval I, accounted for 7.5%, all of which were concentrated within the range of $1/4\,L_T$–L_T downstream of the Sedongpu natural dam, and most of them were boulder bars that were newly formed after the outburst flood. The boulder bars at $\lambda \in [2.66, 14.92]$, accounting for 70% and falling in interval II, were distributed throughout the entire study area. The boulder bars had large λ values within the range of ([14.92, 23.86]), accounting for 22.5% and falling in interval III, and were distributed within $1/4\,L_T$–L_T of the downstream reach length of the natural dam in the curved part of the river channel.

When comparing the size characteristics of the boulder bars before and after the failure of the Sedongpu natural dam, it can be found that the λ values of the boulder bars in the whole study area changed little after the dam failure, except for the large λ values in the purple area in the figure. In addition, the fitting lines are approximately the same (slope and intercept of the line) for all the data before and after dam failure. This means that the outburst flood did not change the relationship between the lengths and widths of boulder bars.

3.3. The Relationship between the Perimeters and Lengths of the Boulder Bars

Based on the λ_b values for the three intervals in Figure 2, the relationship of α-λ, which is the relationship between the perimeters and lengths of the boulder bars, was also divided into three intervals before and after the Sedongpu natural dam failure (Figure 3). The figure shows that except for interval III, α changed little before and after the dam failure for the corresponding intervals. The perimeters in interval III decreased after the dam failure. However, the percentage of boulder bars in this interval was much smaller than the sum of the other two intervals.
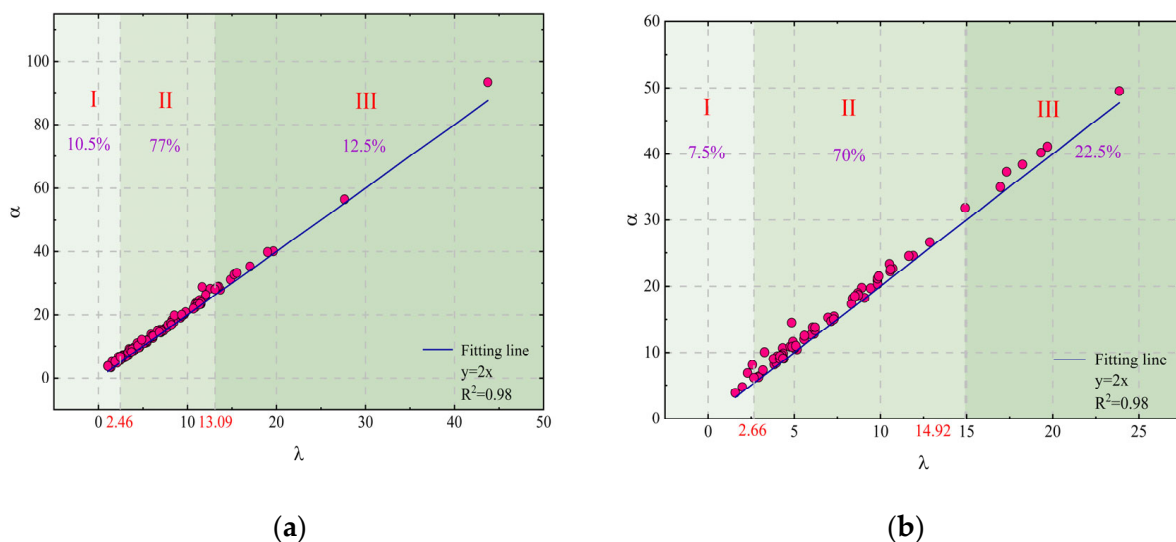

Figure 3. The relationship between λ and α. (**a**) Before the natural dam failure and (**b**) after the natural dam failure. The red dots in the figure represent the field data about the 171 collected boulder bars in study area. The red fonts along X-axis are the boundary values for different intervals. The I, II, and III are the intervals as shown in Figure 2 and the numbers 10.5%, 77%, 12.5%, 7.5%,70%, and 22.5% are the proportions for the corresponding intervals.

The linear relationship between λ and α was the same before and after the failure (i.e., slope of the line and the intercept at the origin), although the upper and lower limits of α and λ of different intervals shifted towards a bit higher value after the failure. This means

that the relationship between the perimeters and lengths was not affected by the outburst flood and follow a linear relationship in the form of Equation (6):

$$P = 2L \tag{6}$$

The Equation (6) suggests that the boulder bars were "self-similar" both before and after the natural dam failure. Specifically, the result indicates that the boulder bars conserved self-similar morphology features after the sudden outburst flood. This adds to the previous observations of the lack of transient river dynamics records. To further investigate self-similarity, the relationship between the number of boulder bars whose perimeters were larger than P and P was investigated (Figure 4) [20]. This showed that there is a power–law relationship between the number of boulder bars with perimeters greater than P and P. This power distribution is equivalent to a fractal distribution [20], which proves the self-similarity of the boulder bars.
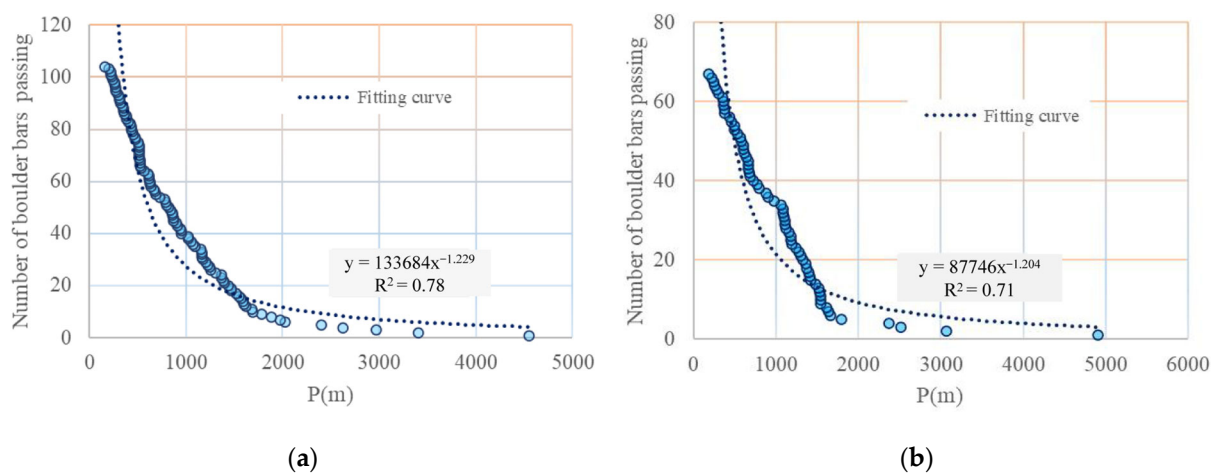

(a)　　　　　　　　　　　　　　　　　　　　　　　　**(b)**

Figure 4. The relationship between the number of boulder bars with a perimeter greater than P and P (**a**) before the failure of the Sedongpu natural dam and (**b**) after the failure of the Sedongpu natural dam. The dots in the figure represent the field data about the 171 collected boulder bars in study area.

3.4. Relationship between Boulder Bar Areas and Lengths

Based on the above analysis, it found that the lengths of the boulder bars determine their perimeters. To explore whether the boulder bar lengths are also a key parameter affecting the boulder bar area (A), we used the correlation coefficient to analyze the degree of correlation between the areas, lengths and widths of the boulder bars.

According to Equation (4), before and after the dam failure, the correlation coefficient P_{XY} for areas, lengths and widths were high. This means that the boulder bar areas before and after the dam failure were more related to the lengths.

The relationship between β and λ is shown in Figure 5, which reflects the relationship between the boulder bar areas and lengths. Three partitions are defined based on the values of λ_b before and after the failure of the Sedongpu natural dam, as above in Figure 2. The figure shows that except for interval III, β changed little before and after the dam failure for the corresponding intervals. The boulder bar areas in interval III decreased after the dam failure. However, the percentage of boulder bars in this interval was much smaller than the sum of the other two intervals. There is a nonlinear relationship between β and λ before and after the dam failure, which can be described by a power exponential function, namely Equation (7):
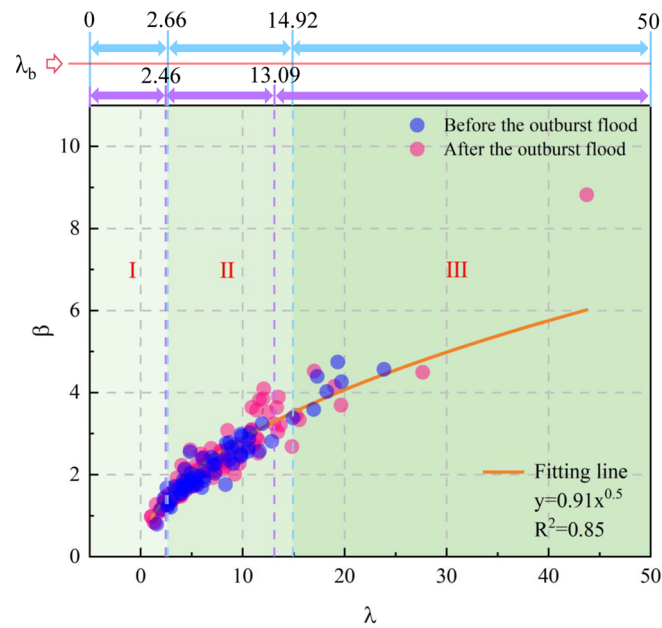
$$\beta = 0.91\lambda^{0.5} \tag{7}$$

Figure 5. The relationship between β and λ. The dots in the figure represent the field data about the 171 collected boulder bars in study area. The I, II, and III are the intervals as shown in Figure 2.

This equation is applicable to λ values with a range of 0–45. The equation provides a quantitative method for calculating the boulder bar areas. In addition, the power exponent equation between β and λ before and after the dam failure remained unchanged, which suggests a fractal relationship. This indicates the self-similar shapes of the boulder bars before and after the natural dam failure, which coincides with the results in Section 3.3.

To analyze the characteristics of the distributions of the number of boulder bars in the study area, we divided the river course into ten sections with lengths of 17.3 km each (Figure 6). Before the dam failure, the number of boulder bars was the largest at 0–17.3 km, i.e., 24 within the section. In addition, the number was the smallest, i.e., 2, at 69.2–86.5 km within the section. After the dam failure, the number of boulder bars was the largest, i.e., 17, at 86.5–103.9 km, and the number was the smallest, i.e., 2, at 121.2–138.5 km.
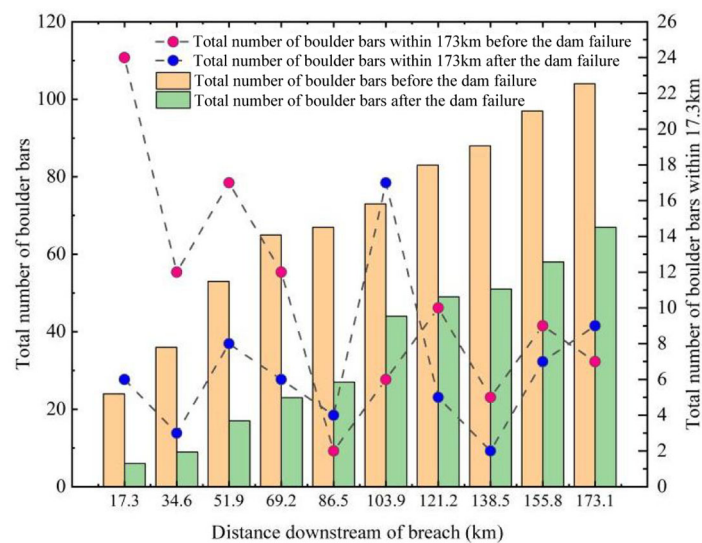

Figure 6. Changes in the number of boulder bars. The left longitudinal axis corresponds to the bar graph and the right longitudinal axis corresponds to the line graph.

In addition, the number of boulder bars after the dam break was significantly smaller than that before the dam break, with a total decrease of 37. This indicates that the number of boulder bars was affected by the outburst flood. By comparison, the number of boulder bars decreased the most, by 18, within 0–17.3 km. Therefore, there is a pattern: as the distance from the dam increased, the decrease in the number of boulder bars became smaller. This suggests that the impact of outburst floods on the number of boulder bars is strongest near the dam.

3.5. Evolution Modes of Boulder Bars

The evolution of boulder bars that are affected by outburst floods can generally be categorized into four modes, as shown in Figure 7. Mode 1 shows that the original boulder bars disappeared after the outburst floods. This mode mostly occurs in the straight segments of the channel. When the outburst flood flows through a straight channel portion, some sediments in the boulder bars are carried away, causing the disappearance of boulder bars.

Mode 2 suggests that the boulder bars were displaced by the outburst flood. In this mode, the shapes and sizes of the boulder bars were similar before and after the dam failure, and the variations in area were less than 10% of the original boulder bars. Mode 3 means that the boulder bars were synthesized from multiple boulder bars into one by the outburst flood. This mode mainly occurred on the convex banks of river bends. Mode 4 indicates that the sizes of the boulder bars decreased due to outburst floods. However, in this mode, the reduction of area of the boulder bars affected by floods was small, i.e., generally less than 10% of the original boulder bars.
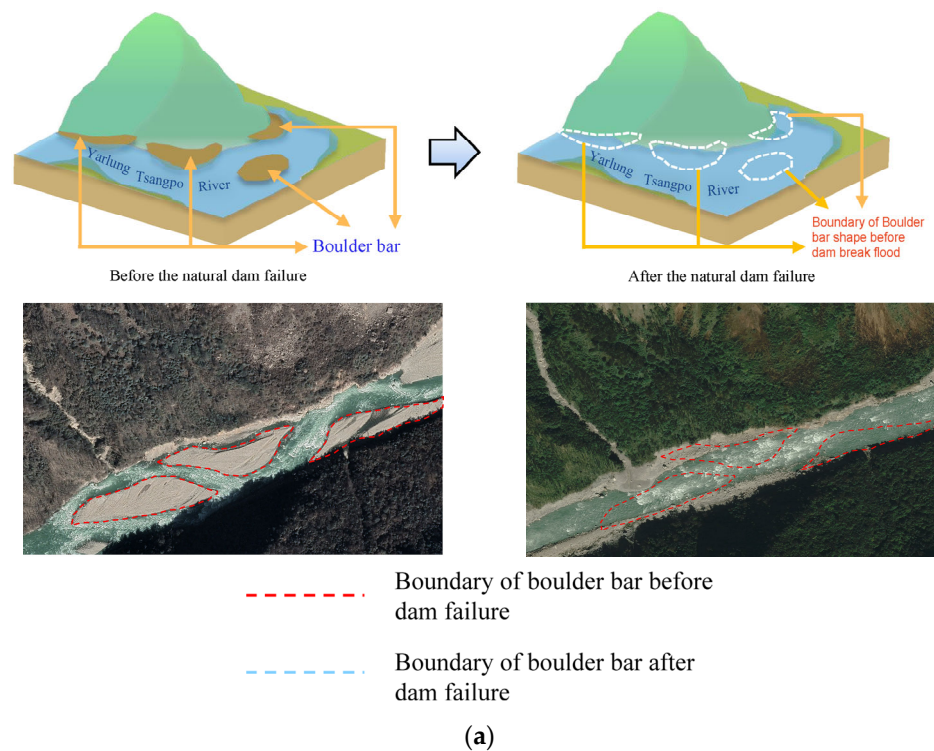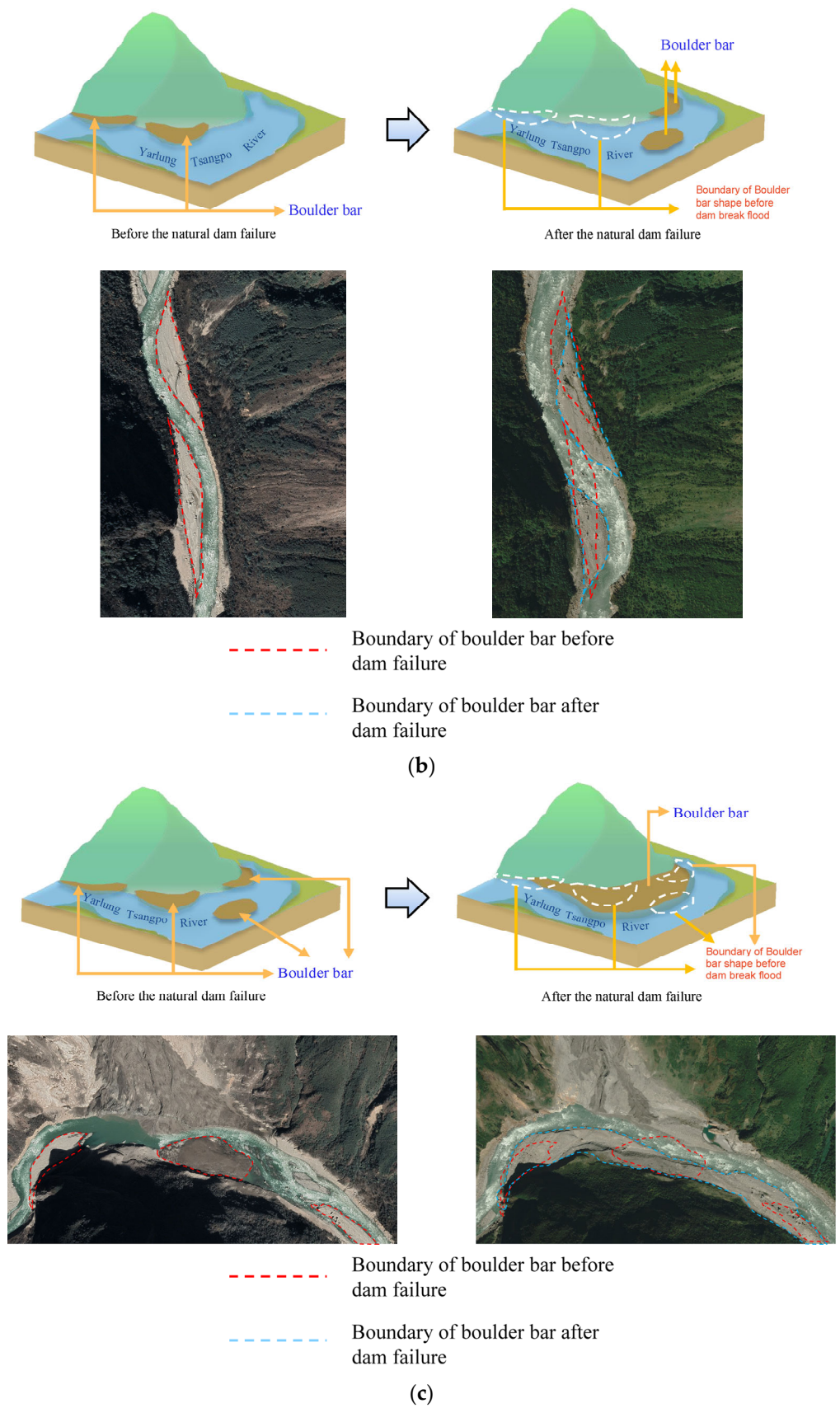

(**a**)

Figure 7. *Cont.*

Boundary of boulder bar before
dam failure

Boundary of boulder bar after
dam failure

(**b**)

Boundary of boulder bar before
dam failure

Boundary of boulder bar after
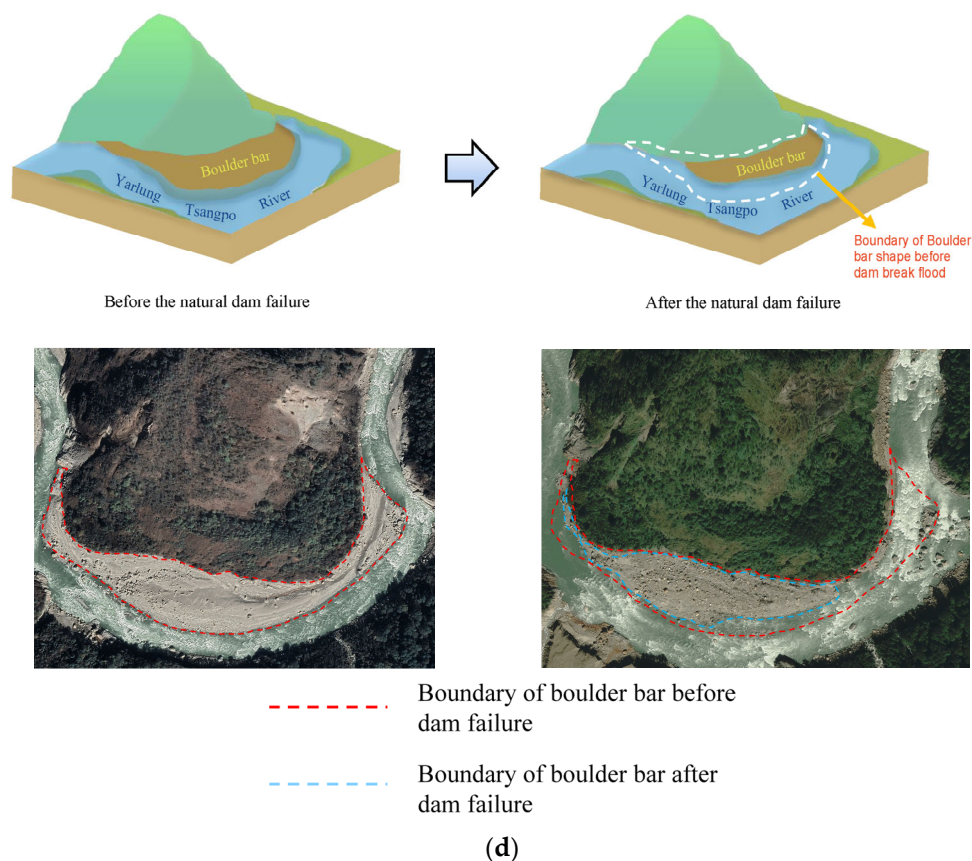dam failure

(**c**)

Figure 7. *Cont.*

Figure 7. The boulder bar evolution modes that are triggered by outburst floods. (**a**) Mode 1: the original boulder bars disappear when triggered by outburst floods. (**b**) Mode 2: the boulder bars are displaced by the outburst flood. (**c**) Mode 3: the boulder bars are synthesized from multiple boulder bars into one by the outburst flood. (**d**) Mode 4: the boulder bar sizes decrease due to outburst floods. The images are Landsat 8 remote sensing images from Google Earth (https://earth.google.com/web/ (accessed on 20 January 2024)).

4. Discussion

4.1. Limitations and Future Work

This paper provides considerable data on boulder bars before and after a landslide dam failure. In the literature, there are many cases of successive landslide dam failures at the same landslide or debris-blocked location. In such conditions, the geometric sizes of the boulder bars would change many times due to many outburst floods. The results in this paper may also apply to such conditions. We need more data about these conditions to verify this. In addition, the boulder bars that were investigated in this study were located no more than 173 km from the landslide dam. However, the results for boulder bars that fall outside of this range are uncertain. Another interesting question is to what extent the outburst flood influences the morphology of the downstream boulder bars. This question can be investigated in the future.

4.2. Self-Similarity of Boulder Bars

In this paper, the self-similarity characteristics of boulder bars before and after a landslide dam failure downstream based on field data are revealed. To further validate this self-similarity relationship, the experimental data of boulder bars from Jiang et al. [10] and field data from Wu et al. [11] are used here. In the experiments conducted by Jiang et al. [10], eight sets of dam failure tests were performed to investigate the formation and morphology of boulder bars located downstream after dam failures. Experimental data, such as the lengths, widths, perimeters and areas of 38 gravel bars, were collected.

Wu et al. [11] conducted field surveys and remote sensing interpretations to evaluate the geomorphological and sedimentary characteristics of the downstream riverbed that was affected by the Yigong landslide dam failure in 2000. They gathered geometric data of 16 boulder bars, including their distances from the landslide dam location, perimeters, areas, lengths and widths.

Figure 8a shows that there is a linear relationship between α and λ based on the experimental data from Jiang et al. [10]. Figure 8b illustrates the relationship between α and λ for the boulder bars, which reveals a linear relationship between the perimeters and lengths of the boulder bars based on the field data from Wu et al. [11]. Figure 9a represents an exponential function relationship between β and λ for experimental data from Jiang et al. [10]. Figure 9b shows the relationship between β and λ for the field data from Wu et al. [11], which indicates that an exponential function relationship existed between the areas and lengths of the boulder bars.
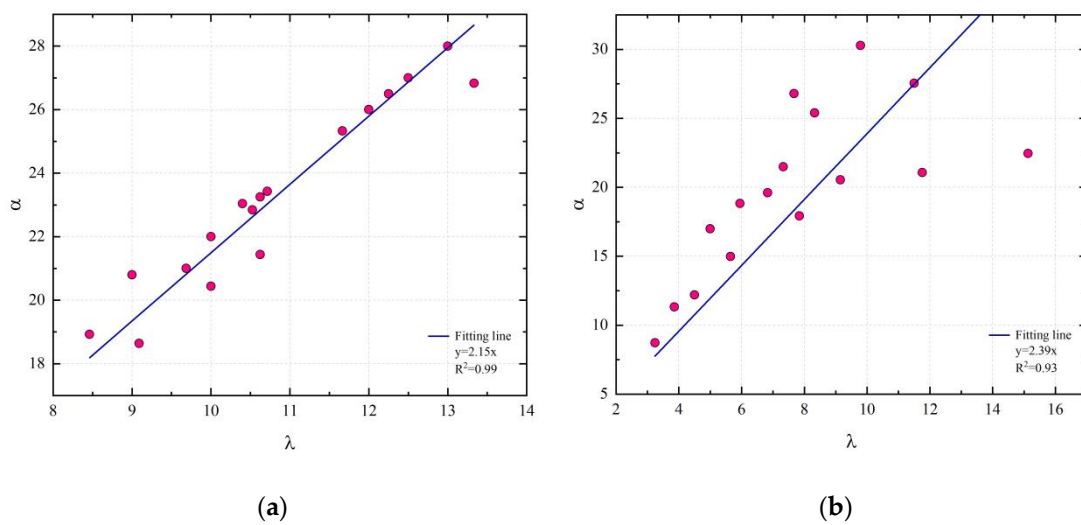

Figure 8. The relationship between λ and α. (**a**) Experimental flume data of Jiang et al. [10]. The red dots in the figure stand for the experimental data (**b**) Field observation data of Wu et al. [11]. The red dots in the figure stand for the field data.
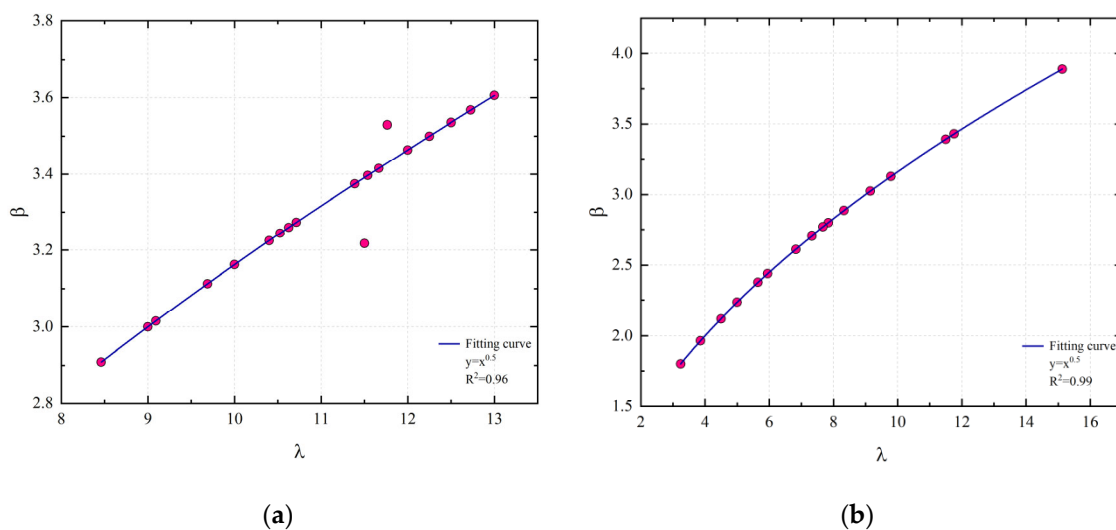

Figure 9. The relationship between β and λ. (**a**) Experimental flume data of Jiang et al. [10]. The red dots in the figure stand for the experimental data (**b**) Field observation data of Wu et al. [11]. The red dots in the figure stand for the field data.

These results indicate that these boulder bars showed self-similar characteristics in the laboratory, which aligns with the findings of the present study. Furthermore, the results also suggest that self-similarity exists in the downstream boulder bars formed after the Yigong landslide dam breach, which is consistent with the results of this study.

5. Conclusions

This paper describes a geomorphological study of a 173 km long reach of the Yarlung Tsangpo River that is located downstream of the Sedongpu natural dam with a particular focus on the changes in the sizes and shapes of boulder bars before and after the failure of the dam. The main conclusions are as follows:

(1) The outburst flood significantly influenced the sizes of boulder bars, yet conserved the similar relationships between the lengths and widths, perimeters and lengths and areas and lengths of the boulder bars in the study area, which reflected the self-similar nature of the boulder bars, as has been reported in some earlier studies. Furthermore, there is a linear relationship between the lengths and widths, perimeters and lengths of boulder bars and a power exponential function for the areas and lengths of the boulder bars that reflects a fractal relationship.

(2) The boulder bars before and after the collapse can be categorized into three shapes: sickle, bamboo leaf and ellipse. The sickle shape is mostly located in curved river sections; the bamboo leaf shape is a stable shape of boulder bars; and the ellipse shape is an early form of boulder bars. The boulder bar shapes changed little from before the failure of the natural dam to after the failure of the natural dam.

(3) After the dam failure, the number of boulder bars decreased with increasing distance from the dam, and the number of boulder bars every 17.3 km first increased and then decreased with increasing distance from the dam.

(4) The changes in the boulder bars caused by the outburst of the dammed lake can be divided into four modes: boulder bars that were washed away from their original positions by the outburst flood (Mode 1), boulder bars that were displaced from their original positions due to the impact of the flood (Mode 2), boulder bars from multiple different original locations that were merged into one by the outburst flood (Mode 3), and large boulder bars that were washed away from their original location by the flood and decreased in size (Mode 4).

Author Contributions: X.J.: Conceptualization; Formal analysis; Funding acquisition; Methodology; Project administration; Resources; Supervision; Visualization; and Writing—review and editing. X.X.: Data curation; Investigation; Methodology; Software; Validation; Visualization; Roles/Writing—original draft; and Writing—review and editing. Z.G.: Data curation; Investigation; Methodology; Software; Validation; Visualization; and Roles/Writing—original draft. A.W.: Conceptualization; Formal analysis; Visualization; and Writing—review. X.L.: Conceptualization; Formal analysis; and Investigation. W.L.: Conceptualization and Formal analysis. Y.X.: Conceptualization and Formal analysis. All authors have read and agreed to the published version of the manuscript.

Data Availability Statement: (a) The digital elevation model (DEM) elevation data were obtained from https://www.gscloud.cn/search (accessed on 21 January 2024). The type of DEM was GDEMV2 30M resolution digital elevation data. (b) The length, width, perimeter and area of the boulder bars in Yarlung Tsangpo River were derived based on Landsat 8 imagery data from October 2018 and October 2020a. These data were obtained from Google Earth Pro software (Version number: 7.3.6.9796), which was downloaded from https://earth.google.com/web (accessed on 21 January 2024).

Conflicts of Interest: Author Xiangang Jiang was employed by the company PowerChina Kunming Engineering Co., Ltd. The remaining authors declare that the research was conducted in the absence of any commercial or financial relationships that could be construed as a potential conflict of interest.

References

1. Gao, Y.; Zhao, S.; Deng, J.; Yu, Z.; Rahman, M. Flood assessment and early warning of the reoccurrence of river blockage at the Baige landslide. *J. Geogr. Sci.* **2021**, *31*, 1694–1712. [CrossRef]
2. Latrubesse, E.M.; Park, E.; Sieh, K.; Dang, T.; Lin, Y.N.; Yun, S. Dam failure and a catastrophic flood in the Mekong basin (Bolaven Plateau), southern Laos, 2018. *Geomorphology* **2020**, *362*, 107221. [CrossRef]
3. Liu, J.J.; Cheng, Z.L.; Li, Y. The 1988 glacial lake outburst flood in Guangxieco Lake, Tibet, China. *Nat. Hazards Earth Syst. Sci.* **2014**, *14*, 3065–3075. [CrossRef]
4. Shrestha, B.B.; Nakagawa, H. Assessment of potential outburst floods from the Tsho Rolpa glacial lake in Nepal. *Nat. Hazards* **2014**, *71*, 913–936. [CrossRef]
5. Yan, K.; Zhao, T.; Liu, Y. Experimental investigations on the spillway section shape of the breaching process of landslide dams. *Int. J. Geomech.* **2022**, *22*, 04022045. [CrossRef]
6. Turzewski, M.D.; Huntington, K.W.; LeVeque, R.J. The geomorphic impact of outburst floods: Integrating observations and numerical simulations of the 2000 Yigong flood, eastern Himalaya. *J. Geophys. Res. Earth Surf.* **2019**, *124*, 1056–1079. [CrossRef]
7. Carrivick, J.L.; Jones, R.; Keevil, G. Experimental insights on geomorphological processes within dam break outburst floods. *J. Hydrol.* **2011**, *408*, 153–163. [CrossRef]
8. Chen, R.; Chen, J.; Ma, J.; Cui, Z. Quartz grain surface microtextures of dam-break flood deposits from a landslide-dammed lake: A case study. *Sediment. Geol.* **2019**, *383*, 238–247. [CrossRef]
9. Hanson, M.A.; Clague, J.J. Record of glacial Lake Missoula floods in glacial Lake Columbia, Washington. *Quat. Sci. Rev.* **2016**, *133*, 62–76. [CrossRef]
10. Jiang, X.; Cheng, H.; Gao, L.; Liu, W. The formation and geometry characteristics of boulder bars due to outburst floods triggered by overtopped landslide dam failure. *Earth Surf. Dyn.* **2021**, *9*, 1263–1277. [CrossRef]
11. Wu, C.; Hu, K.; Liu, W.; Wang, H.; Hu, X.; Zhang, X. Morpho-sedimentary and stratigraphic characteristics of the 2000 Yigong River landslide dam outburst flood deposits, eastern Tibetan Plateau. *Geomorphology* **2020**, *367*, 107293. [CrossRef]
12. Billi, P. Channel processes and sedimentology of a boulder-bed ephemeral stream in the western Afar margin. *Z. Für Geomorphol.* **2016**, *60*, 35–52. [CrossRef]
13. Guan, M.; Wright, N.G.; Sleigh, P.A.; Carrivick, J.L. Assessment of hydro-morphodynamic modelling and geomorphological impacts of a sediment-charged jökulhlaup, at Sólheimajökull, Iceland. *J. Hydrol.* **2015**, *530*, 336–349. [CrossRef]
14. Guan, M.; Wright, N.G.; Sleigh, P.A. Multiple effects of sediment transport and geomorphic processes within flood events: Modelling and understanding. *Int. J. Sediment Res.* **2015**, *30*, 371–381. [CrossRef]
15. Mandelbrot, B.B. The Fractal Geometry of Nature/Revised and Enlarged Edition. New York. 1983. Available online: https://ui.adsabs.harvard.edu/ (accessed on 21 January 2024).
16. Nikora, V.I. Fractal structures of river plan forms. *Water Resour. Res.* **1991**, *27*, 1327–1333. [CrossRef]
17. Daly, E.; Porporato, A. Some self-similar solutions in river morphodynamics. *Water Resour. Res.* **2005**, *41*, 1–5. [CrossRef]
18. An, B.; Wang, W.; Yang, W.; Wu, G.; Guo, Y.; Zhu, H.; Gao, Y.; Bai, L.; Zhang, F.; Zeng, C.; et al. Process, mechanisms, and early warning of glacier collapse-induced river blocking disasters in the Yarlung Tsangpo Grand Canyon, southeastern Tibetan Plateau. *Sci. Total Environ.* **2022**, *816*, 151652. [CrossRef] [PubMed]
19. Liu, C.; Lü, J.; Tong, L.; Chen, H.; Liu, Q.; Xiao, R.; Tu, J. Research on glacial/rock fall-landslide-debris flows in Sedongpu basin along Yarlung Zangbo River in Tibet. *Geol. China* **2019**, *46*, 219–234. (In Chinese with English abstract) [CrossRef]
20. Turcotte, D.L. Fractals and fragmentation. *J. Geophys. Res. Solid Earth* **1986**, *91*, 1921–1926. [CrossRef]